Cooling Power Electronic Building Blocks Aboard Navy Ships

by

Joushua Padilla

Submitted to the Department of Mechanical Engineering in Partial Fulfillment of the Requirements for the Degree of

Bachelor of Science in Mechanical Engineering

at the

Massachusetts Institute of Technology

June 2021

© 2021 Massachusetts Institute of Technology. All rights reserved.

Signature of Author:	
	Department of Mechanical Engineering
	May 14, 2021
Certified by:	
	Chryssostomos Chryssostomidis
	Professor of Mechanical and Ocean Engineering
	Department of Mechanical Engineering
	Thesis Supervisor
Accepted by:	
	Kenneth Kamrin
	Associate Professor of Mechanical Engineering
	Undergraduate Officer

Cooling Power Electronic Building Blocks Aboard Navy Ships

by

Joushua Padilla

Submitted to the Department of Mechanical Engineering on May 14, 2021 in Partial Fulfillment of the Requirements for the Degree of

Bachelor of Science in Mechanical Engineering

ABSTRACT

The Navy Integrated Power and Energy Corridor (NiPEC) is a modular entity that encapsulates all the power handling requirements of a shipboard power and energy distribution system including transmission, conversion, protection, isolation, control and storage. The basic component of the NiPEC is the Power Electronics Building Block (PEBB), which is envisioned to be a universal converter that is programmed for the specific application when installed. The PEBB is a modular unit that can be easily swapped out and is small and light enough to be carried and installed by a single person. One constraint placed on the PEBB to ensure ease of swapping is that no liquid can cross the boundary of the PEBB, thus eliminating the possibility of leaking at the interface.

This thesis describes the design and analysis of a system for removing up to 10 kW of heat from each PEBB in a stack of four PEBB units, using liquid cooling via a dry interface. This is achieved by hard-mounting cold plates in the electronics cabinet, placing the heat-transfer surface of each PEBB adjacent to a cold plate, and improving heat transfer across the interface through the use of a thermal pad. The thesis presents initial thermal and structural analyses using analytical models, computational fluid dynamics and mechanical design tenets. These analyses demonstrate that this is a viable solution to the PEBB cooling problem.

Thesis Supervisor: Chryssostomos Chryssostomidis Title: Professor of Mechanical and Ocean Engineering

Acknowledgements

I would like to thank Dr. Consi, Dr. Chalfant, and Professor Chryssostomidis, for their guidance and help throughout the course of this project. I would also like to thank the project's sponsors, MIT Sea Grant and the Office of Naval Research, as well as my parents for their support throughout my education.

Table of Contents

Ab	ostract	2
Ac	cknowledgements	4
Ta	able of Contents	5
Lis	st of Figures	6
Lis	st of Tables	7
1.	Introduction	8
2.	Background	10
3.	Analytical Models	16
4.	Simulated Models	28
5.	Results and Discussion	35
6.	Conclusion	36
7.	References	38

List of Figures

Figure 1: PEBB stack structure including proposed cooling design	9
Figure 2: PEBB's Full Bridge including 72 dice split into groups of six	10
Figure 3: Image of typical silicon based high conductivity thermal pad	11
Figure 4: Diagram showing thermal pads ability to lower contact thermal resistance	12
Figure 5: CAD image of cold plate for proposed liquid cooling design	13
Figure 6: CAD image of cold plate, thermal pad, and PEBB's Dice used in CFD modeling.	15
Figure 7: Diagram showing components of air-cooling system used currently for testing.	16
Figure 8: Thermal resistance diagram of air-cooled solution including PEBB and heatsink	17
Figure 9: Diagram of liquid-cooling proposed design	17
Figure 10: Thermal resistance diagram of liquid-cooling proposed solution	18
Figure 11: Diagram showing effect of heat spreading angle	19
Figure 12: Static load simulation result of pressure on cold plate	22
Figure 13: Plot showing effect of pressure on thermal pad's thermal resistance	23
Figure 14: CFD result of water cooling under uniform thermal load	31
Figure 15: CFD result of water cooling under Nonuniform thermal load	32
Figure 16: CFD result of refrigerant cooling under Nonuniform thermal load	33
Figure 17: CFD result of refrigerant cooling under uniform thermal load	34

List of Tables

Table 1: Critical values and conditions of cold plates analytical modeling	26
Table 2: Analytical model's thermal resistance results for water and R-134a	28
Table 3: Boundary conditions and initial conditions of CFD simulations	29
Table 4: CFD simulation's thermal resistance results for water and R-134a	30
Table 5: Comparison of analytical model's results to CFD simulation results	35
Table 6: Comparison of liquid-cooling effectiveness to air-cooling effectiveness	36

1. Introduction

The Navy's Electric Ship Research Design Consortium (ESRDC) works to advance technologies and concepts for an electric ship. A part of this design involves adding new electronics that must be cooled and arranged according to naval architects' specifications. A solution is needed that extracts 10 kW of heat from large power electronics stacked into arrays aboard these new vessels. Work has been done to explore the potential of cooling systems such as heat sinks and cold plates to cool the large heat load to below 150 degrees Celsius.

The final design must adhere to a multitude of constraints. First, the large heat load means that liquid cooling would be the most effective, however if a liquid cooling design is proposed, it must be leak-proof. Second, each PEBB must be electrically insulated from the rest of the ship. Third, each PEBB must be a maximum of 30 pounds. Fourth, the PEBBs must be low maintenance, allowing sailors aboard the vessel to easily change out a PEBB with minimal training. Finally, each PEBB's critical electronics, also known as dice, must remain under 150 degrees Celsius during the worst-case thermal operation.

Currently to meet these needs, a finned-heat-sink cooling design is used for testing purposes. This design incorporates a large aluminum heat sink that is bolted to the PEBB. The heat is extracted from the dice through conduction and then conducted through the fins as air is pushed across the heat sink and convection cooled. This solution is quite robust and easily implemented however, the use of air as a working fluid limits its effectiveness. Because of system's high heat flux, the current solution cannot support the full 10 kW heat load.

The design that is proposed in this paper is a liquid-cooled design that utilizes heat exchangers, thermal pads, and a new mechanical design that integrates the liquid cooling directly into the stack structure of the PEBBs as seen in Figure 1.

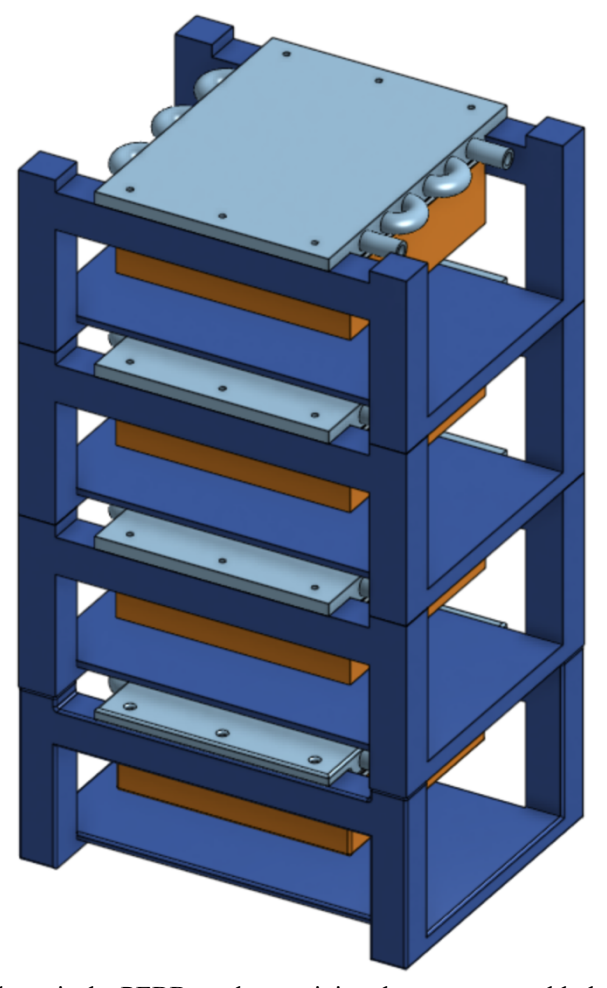


Figure 1: Above is the PEBB stack containing the structure, cold plates, thermal pads and PEBBS.

This integrated liquid cooling plate, or cold plate, does not have to be moved when a PEBB is being replaced, allowing for rigid leak-proof connections. The thermal pads minimize thermal contact resistance between the cooling solution and the electronics. The new cold plate designs, hydrocarbon working fluids, and novel stack structures allow for easy replacement of the PEBBs. This design was evaluated using both analytical heat transfer and thermal-fluids models, as well as using the flow simulation software SIMSCALE. These results were compared to each other and

to the results from the current air-cooled solution. This paper will go into detail about the specifics of the proposed design and the models used to verify the effectiveness of this design.

2. Background

The inner electrical components of a PEBB that must be cooled are called dice. In a full bridge, also known as a module, there are 72 dice arranged in groups of six as seen in Figure 2.

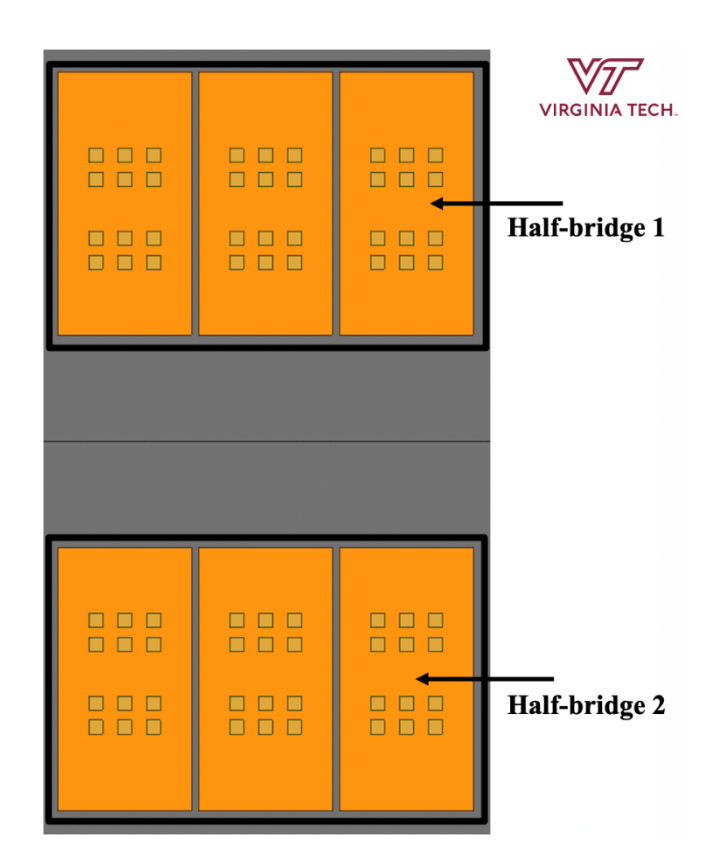


Figure 2: The die grids assembled into two Half-bridges. [6]

Industry specifications dictate that these dice must be kept below 175 degrees Celsius, and after accounting for a safety factor it is typical to set the temperature limit to be 150 degrees Celsius. Each die is 8.1mm by 8.1mm, and is attached to a piece of electrically insulating ceramic.

Although the exact thickness of the die is unknown, the thickness of the ceramic between the die and the top of the PEBB is 7.5mm. This thickness means that some level of heat spreading will occur within the ceramic plate ensuring that the heat does not remain in the die. Each die has a thermal resistance of 0.4 K/W from the junction to the outside of the ceramic plate. This relatively high thermal resistance means that the cooling solution must remove heat quickly to ensure that overheating does not occur. Adding a thermal pad ensures a good thermal connection between the PEBB and cooling solution.

Thermal pads are commonly used to lower the contact resistance between an electronic component and a cooling solution. Thermal pads are silicon-based and have thermally conductive material embedded in them to ensure low thermal resistance. A generic thermal pad can be seen in Figure 3.



Figure 3: A typical high conductivity thermal pad.

Thermal pads lower the contact resistance by filling interstitial gaps that are inherently formed when two pieces of flat material are pressed together at a pressure of between 10 psi and 30 psi.

This compressive force causes 3-dimensional displacements to occur in the material of the thermal pad. The moving material fills the small gaps between the electronic and cooling solution, introducing a new conductive pathway between the two. This decreases the thermal contact resistance and increases the effectiveness of the cooling solution [1]. A diagram of this gap filling process can be seen in Figure 4.

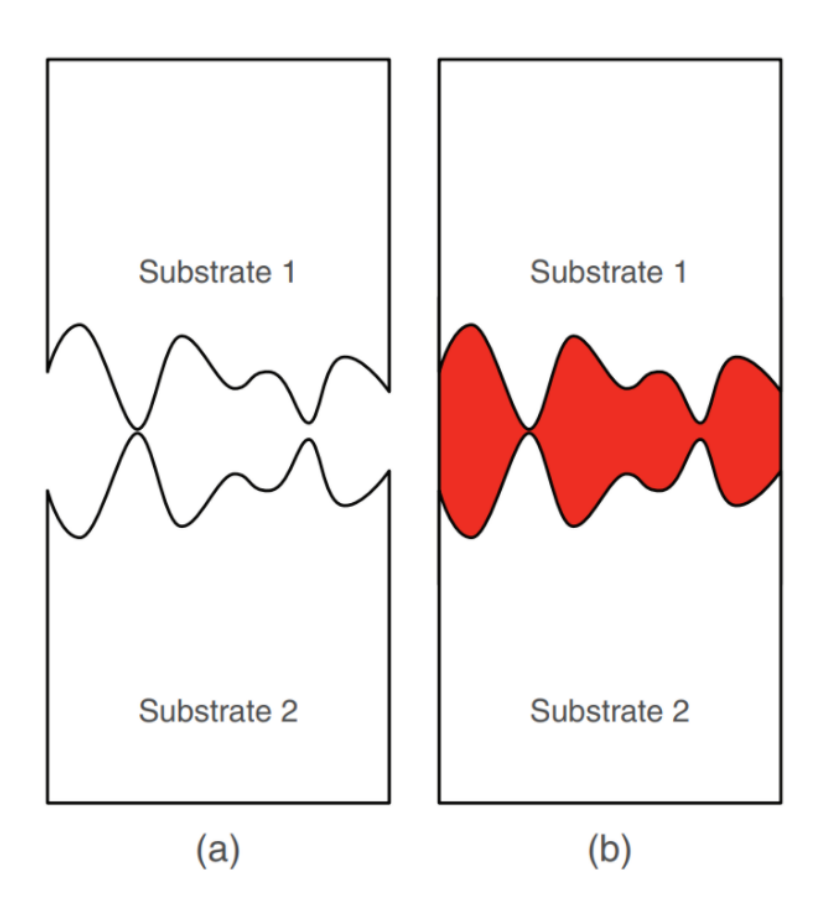


Figure 4: Above demonstrates how a thermal pad (represented by red material in right-hand image) fills the interstitial gaps between two solid materials [1].

Thermal pads are normally very thin, between 0.5mm and 2mm in thickness, and come in a range of conductivities. The higher conductivity thermal pads range between 6 W/m-K to 18 W/m-

K. Specifically, this proposed design included a 2mm, 17.8 W/m-K thermal pad, allowing for a very low thermal resistance between the liquid cooling plate and PEBB [2].

Due to the high heat loads that must be dissipated from each PEBB, liquid cooling is the ideal solution. One liquid cooling technology commonly used in industry is a cold plate. Cold plates in their simplest form are made of aluminum stock of a desired thickness inlaid with copper piping. A working fluid, commonly chilled water, is pumped through the copper piping before returning to the chiller to be cooled. The characteristics of cold plates such as low thermal resistance, heat dissipation qualities, and easy customization, mean they are an excellent choice for high heat flux systems like PEBBs. For the proposed design in this paper, the selected cold plate contains two sets of piping run concentrically such that the working fluid in the two sets of piping is pushed in opposite directions. This design forms a concentric, counter flow heat exchanger within the cold plate. This design is seen in Figure 5.

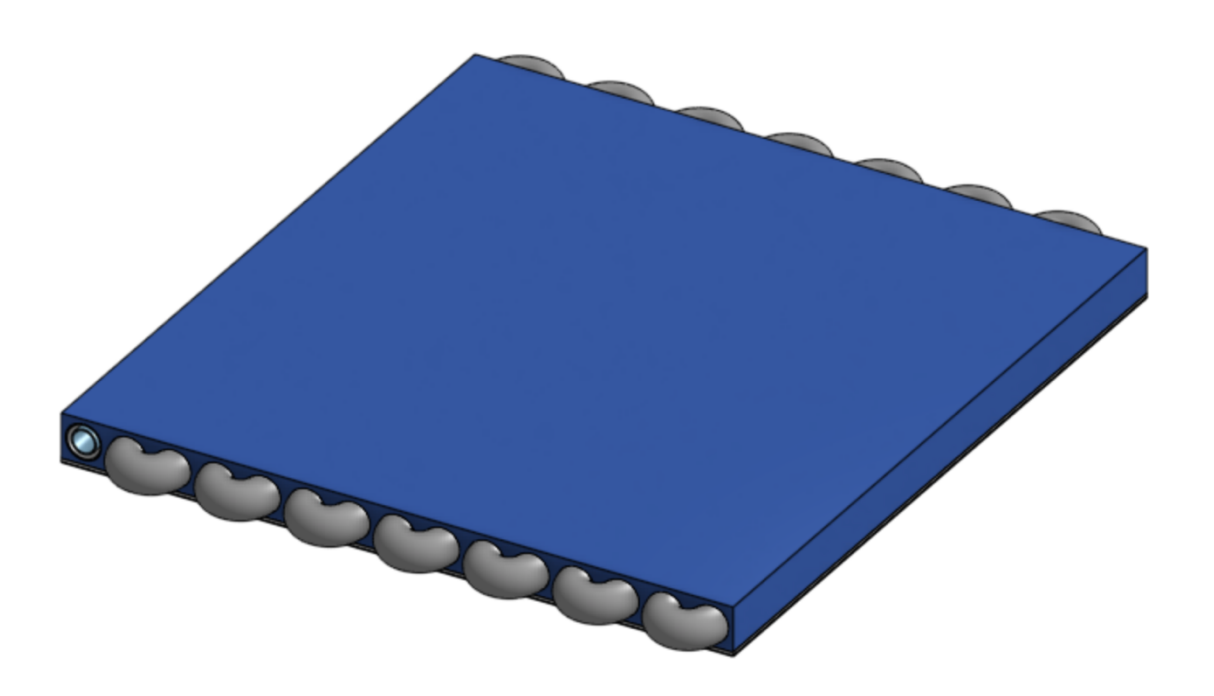


Figure 5: A counter-flow concentric cold plate with ½ inch diameter piping.

The heat exchanger enhances heat transfer qualities within the cold plate, ultimately improving the overall performance of the cooling solution.

One constraint of liquid cooling is the need for the PEBB stack and cooling solution to be electrically isolated from the rest of the ship. To ensure this, electrically isolative fluids such as deionized (DI) water or refrigerants like R-134a must be used. These fluids will alter the thermal performance of the cold plate and must be explored thoroughly using thermal-fluids analysis techniques.

The complete cooling solution that incorporates the ceramic plate, thermal pad, and cold plate is shown in Figure 6.

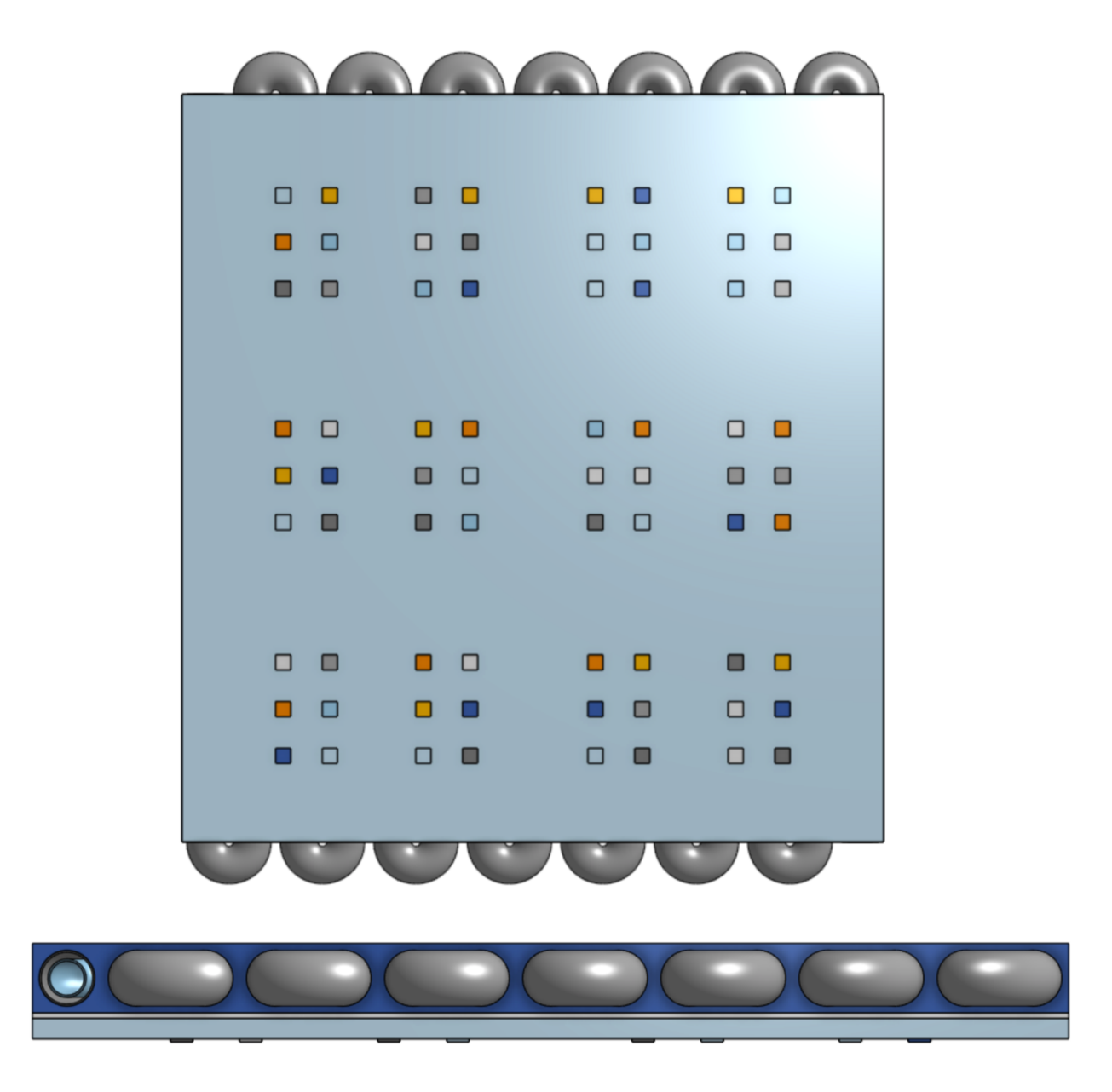


Figure 6: The two images above show the arrangement of the dice relative to the cold plate and thermal pad in plan view (top image) and elevation (bottom image)

The thermal performance of each proposed design component will be evaluated individually in Sections 3 and 4.

3. Analytical Models

The current method for cooling the PEBB during tests uses a combination of a large aluminum heat sink and fans to produce a high convective coefficient around the fins of the heat sink. This robust design is limited in its cooling capacity due to the high power necessary to produce the high convection coefficient and the lower specific heat and density of the working fluid, air, which is limited in its heat transfer abilities. The current setup has been modeled using a simplified one-dimensional thermal resistance network. This network consists of three main thermal resistances: the resistance of the module, R_{module} , which quantifies the thermal resistance of a full bridge of dice to the external case of the PEBB, the resistance of the heat sink, R_{cs} , and the convective resistance from the heat sink fins to the air, R_{sa} . A representation of this cooling solution is seen in Figure 7.

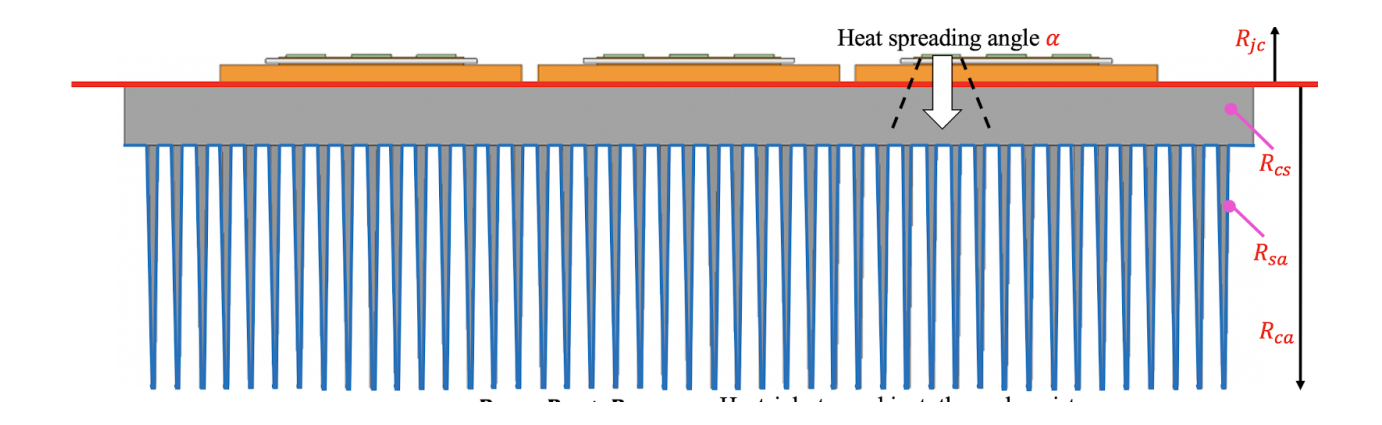


Figure 7: Diagram showing components of air-cooling system used currently. [6]

This setup yields a thermal resistance network as seen below in Figure 8.

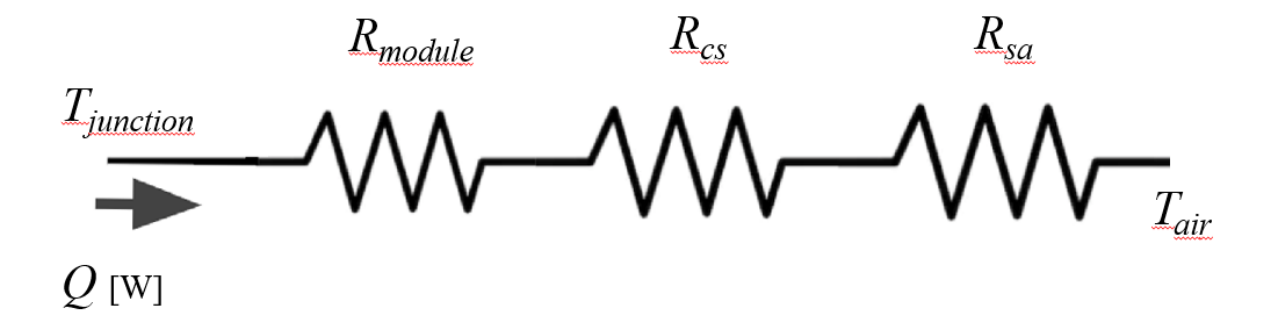


Figure 8: Thermal resistance network of air-cooling system currently used where R_{module} is the resistance of the dice within the PEBB and R_{ja} is the resistance from the dice to the air.

The liquid cooling method being proposed in this paper can be modeled with a similar one-dimensional resistance network. The module resistance remains the same. The thermal resistance of the cold plate is added. The thermal pad introduced between the cooling solution, the cold plate, and the PEBB is put under a considerable amount of pressure, about 10 psi, which ensures a lowered thermal contact resistance between the PEBB and the cold plate. The physical representation of this liquid cooling solution on a single PEBB is seen in Figure 9.



Figure 9: Diagram of proposed liquid-cooled system.

The resistance network of this liquid cooling solution is slightly more complex but it is also more effective; the effectiveness of the cold plate allows for this proposed cooling system to remove much more heat from the PEBB. This network is seen in Figure 10.

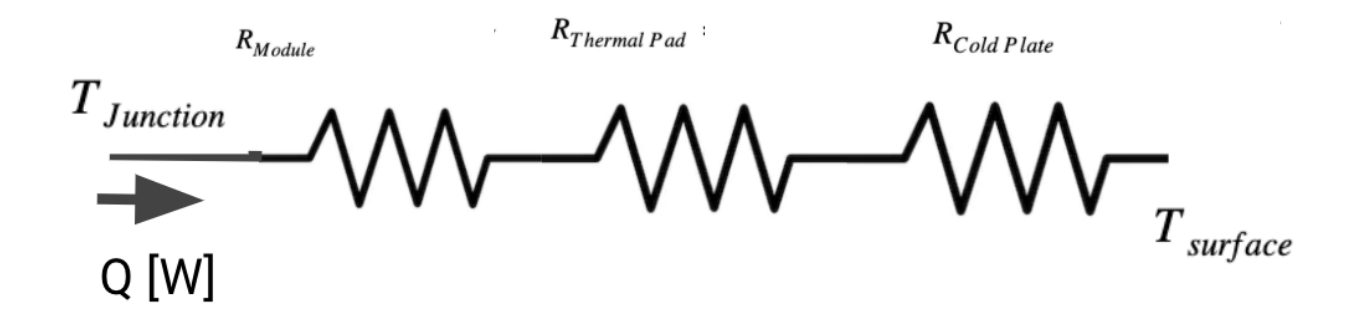


Figure 10: Thermal resistance diagram of proposed liquid-cooling system where R_{module} is the resistance of the dice within the PEBB and $R_{ThermalPad}$ is the resistance of the thermal pad and $R_{ColdPlate}$ is the resistance of the cold plate.

To understand the one-dimensional thermal resistance models, first it is important to understand the steps taken to create the model representing the thermal resistance per die of each module. A module in a PEBB is synonymous for a full bridge. A module consists of 72 dice spread out in groups of six over the structure of the PEBB, in a singular plane. The dice are attached to an electrically insulating ceramic material with a thickness of 7.5mm. This means within the thermal resistance of the module per die, the model must reflect the conductive heat transfer between the die itself and the ceramic layer. First, a ceramic material must be assumed. A common electrically insulating thermally conductive ceramic used in electronics is aluminum nitride, which has a thermal conductivity is 180 W/m-K [3], a die thickness is assumed to be 0.5 mm. This results in a total module thickness of 8 mm. Another assumption that must be made is about the heat spreading angle within the ceramic. The heat spreading angle determines how the heat spreads in

a material from surface to surface. It is commonly used in layered cases such as this one. The heat spreading angle describes the thermal energy's pathway through a material and how that pathway gets larger as the heat begins to spread, as seen in Figure 11 [4].

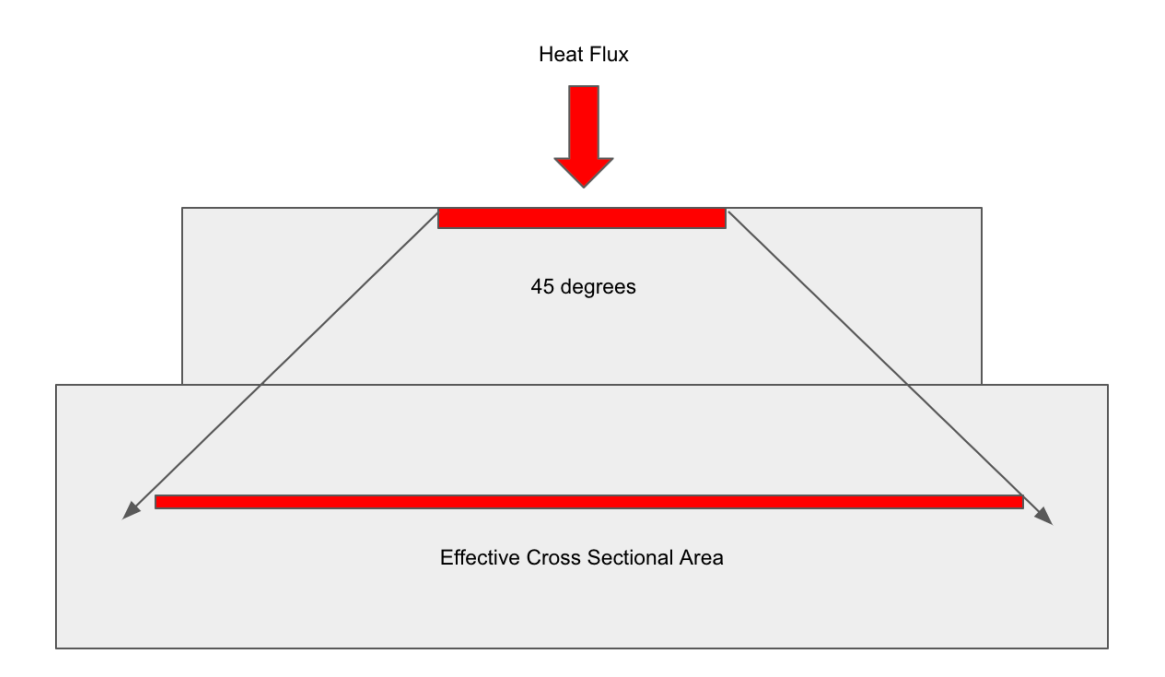


Figure 11: The figure above shows how heat spreading angle changes effective cross-sectional area as a function of height through a material [4].

We assume a heat spreading angle of 45 degrees, which is a typical assumption for the ceramic plate in this model, consistent with [6].

Finally, the thermal resistance network from the die's junction to the ceramic surface can be determined by calculating the thermal resistance of each component and putting them in series. First, the ceramic's thermal resistance, is determined using:

$$R = \frac{L}{KA}[5],\tag{1}$$

where *L* is the critical length, *A* is the effective critical cross-sectional area, and K is the thermal conductivity of the ceramic. *A* is calculated by averaging the cross-sectional area of the heat pathway at the base of the ceramic and that of the pathway at the top of the ceramic. The base area is 6.561E-5 m² and the top area is 0.000534 m². Thus, the known values are: L=0.0075m, A=0.00029805 m², and K=180 W/m-K. This yields a ceramic thermal resistance of 0.139 K/W. Finally, because the total resistance from junction to case per die is known to be 0.4 K/W, the resistance of the die itself is 0.261 K/W.

Next, the resistance of the thermal pad per die must be determined. As said above, thermal pads are inserted between an electronic component that needs to be cooled and the cooling solution such as a heat sink to lower the contact resistance by filling in the small gaps between the surfaces when they are put under a unidirectional compressive load. This compressive load allows for the rubber-like material of the thermal pad to fill the interstitial gaps between the components, supplying a new conductive pathway where an air gap would have been. For the thermal pad to work effectively, a minimum of 10 psi compressive load is recommended to ensure that the gaps are filled. Normally, with small electronic components, 10 psi would not be considered much of an issue, however due to the 16 in by 16 in cross section of a PEBB, to meet the 10 Psi recommendation, 2,560 pounds or 11387.45 N, of force is necessary. To meet this load requirement there will need to be a high force linear actuated option, such as a hydraulic press. A hydraulic press would allow for the required force in a relatively small overall form. While a specific actuator has not been specified in this paper, there are several possible presses that meet the force specification, which suggests this will not be an issue. The large amount of pressure will

not only ensure that there is good thermal contact between the components, but also will also require both the PEBB and cold plate to have the necessary structural strength to prevent failure in the form of buckling and plastic deformation. Specifically, deformation in the cold plate could render the thermal pad ineffective. Both of these issues have been addressed in design and will now be explained in depth.

First, the structure of the PEBB must not fail under a high compressive load, while also meeting the weight constraint of the PEBB of 30 pounds. As a result, the structural walls can be a maximum of seven pounds, thus constraining the PEBB walls to be 0.1 inches thick. Upon further discussions with the team designing the PEBBs at Virginia Tech, the PEBB's overall geometry is still in flux so these calculations are not by any means final. Using these assumptions, the walls of the PEBB were treated as a hollowed out rectangular cross sectioned beam under a compressive load. The failure mode was assumed to be buckling behavior. In buckling failure, a critical axial compressive load must be reached to begin the beams bucking behavior. The critical load of the beam with the 0.1-inch-thick aluminum walls was found using the following [3],

$$P_{critical} = \frac{\pi^2 EI}{4L^2},\tag{2}$$

where $P_{critical}$ is found to be 6.08E8 Newtons, E is Young's modulus of elasticity, I is the area moment of inertia and L is the length of the beam. This calculated critical load is far greater than the load which the press would be enacting on the PEBB's walls.

To address the effect deformation of the cold plate would have on the thermal connection between the thermal pad and cold plate, a simulation was run to identify how the cold plate would deform under a 10 Psi compressive load. The resulting deformation was a curve in the cold plate with maximum deflection of 0.0001m in the middle of the cold plate as seen in Figure 12.

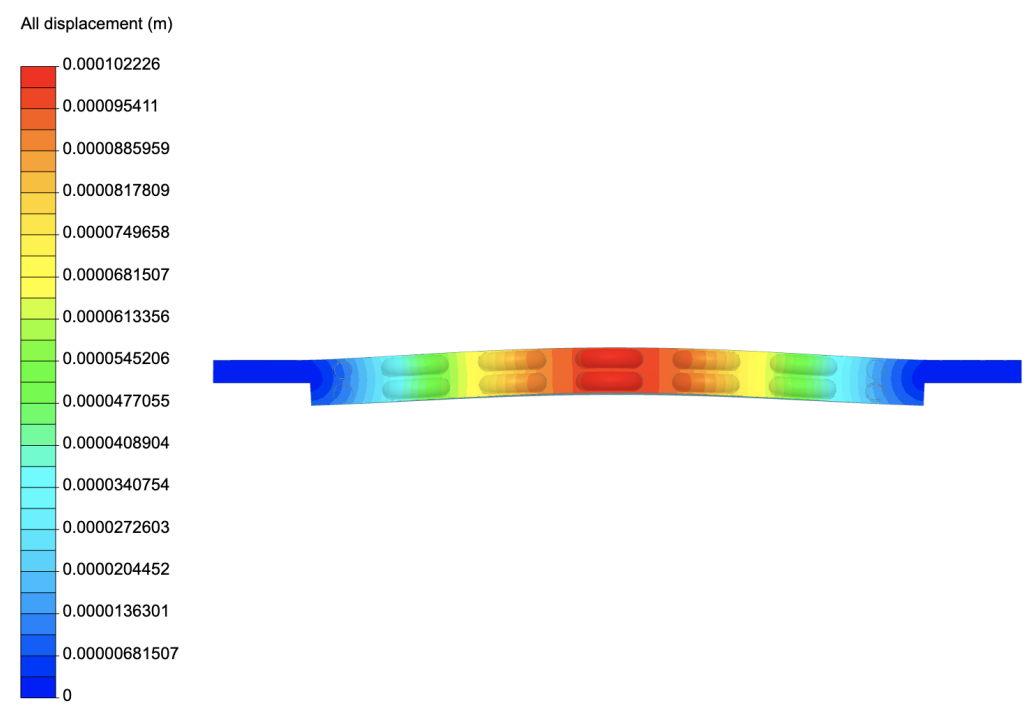


Figure 12: Static simulation results of cold plate deformation due to compressive load. Note that the deformation of the plate is scaled by a factor of 100 in this image for visualization purposes

The deformation in the cold plate, which will result in a loss of compressive deformation in the thermal pad, is found to be negligible. In fact, the 0.0001m deformation in the cold plate only results in a 5% decrease in the nominal deformation of the thermal pad since the thermal pad specified for this design is a 0.002m thick. The deformation in the thermal pad will lead to a fluctuation in the thermal resistance of the pad. However, the very small loss in compressive deformation does not cause considerable fluctuations in thermal resistance or temperature across the width of the thermal pad as represented in Figure 13.

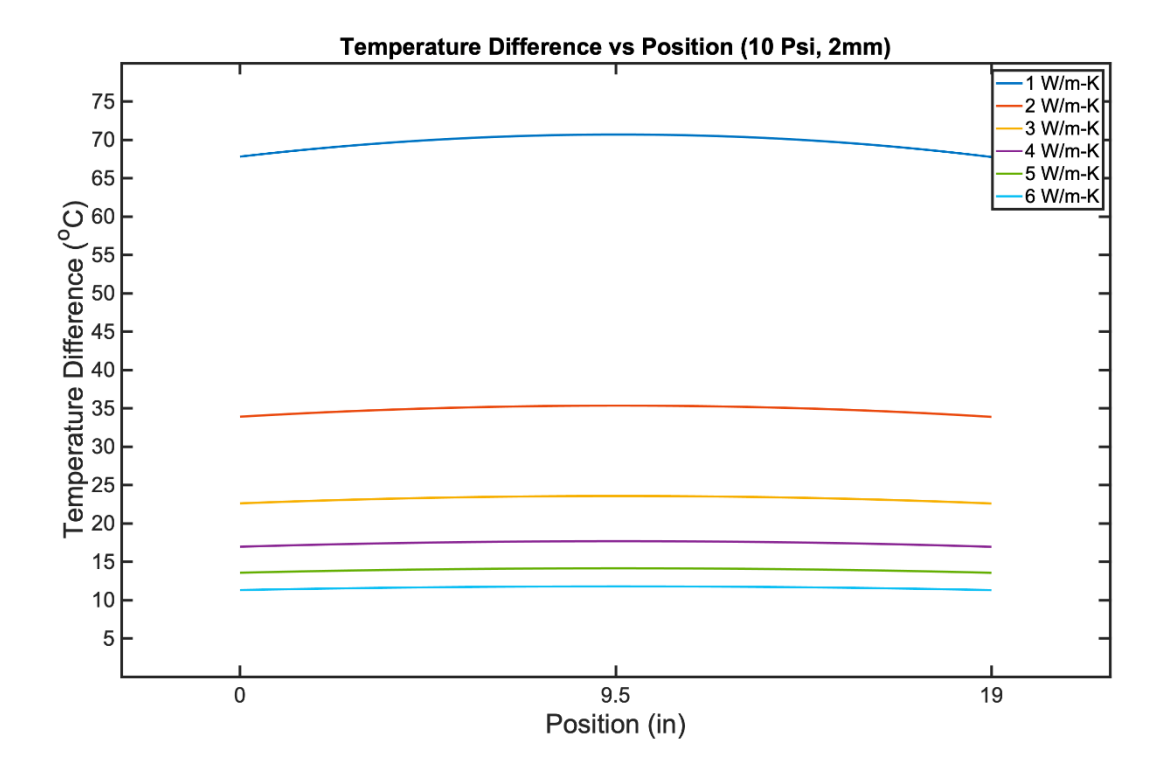


Figure 13: The above plot shows the temperature gradient versus horizontal position along the cold plate at various thermal conductivities. At high thermal conductivities the temperature gradient's dependence on position along the cold plate is negligible.

Figure 13 shows that the deformation due to the compressive load will not cause any sizable fluctuations in thermal conductivity at the interface between the cold plate and thermal pad. Thus, the given conductivity, thickness, and critical cross-sectional area of the thermal pad can be used to find the thermal resistance of the thermal pad. To find the resistance, the same equation, [5]

$$R = \frac{L}{KA}, \tag{1}$$

can be used where the values are: L=0.002 m, A=0.000534 sqm, and K=17.8. This yields a thermal resistance, of 0.21 K/W per die for the thermal pad.

The final component of the resistance network is the cooling solution, which in the case of this proposed system, is a cold plate. The cold plate that was designed for this application utilizes a counter-flow heat exchanger design. This design requires more pumping power and piping but also enables the cold plate to be more effective in cooling the large heat load. To solve for the cold plate's thermal resistance, a Nusselt number analysis must be conducted. First, the Reynolds number, must be calculated using [5],

$$Re = \frac{\rho vD}{\mu},\tag{3}$$

where ρ is the fluid density, v is the fluid velocity, D is the critical length, and μ is the dynamic viscosity of the fluid. The Reynolds number is used to determine whether the flow is in the turbulent or laminar regimes, which will dictate the heat transfer characteristics of the cold plate. Next, the Nusselt number analysis can be used to calculate the heat transfer coefficient of the fluid in the piping of the heat exchanger. Nusselt number can be calculated by using one of two methods. The first is a simpler method [5],

$$Nu = \frac{hD}{K_E},\tag{4}$$

where h is the heat transfer coefficient, D, the critical length and K_F is the conductivity of the fluid. The other method uses an extensive correlation [5],

$$Nu = \frac{(f/8)(Re-1000)Pr}{\frac{1}{1+12.7(\frac{f}{8})^{\frac{1}{2}}(Pr^{\frac{2}{3}}-1)}},$$
(5)

where f is the friction factor of the piping, Re the Reynolds number, and Pr the Prandtl number. The friction factor, f, is solved using [5],

$$f = (0.79 \ln(Re) - 1.64)^{-2}. \tag{6}$$

The lengthy Nusselt correlation, equation 5, can be used with the friction factor relation to solve for the Nusselt number. Then, equations 4 and 5 can be used to solve for the heat transfer coefficient of the fluid, h, passing through the piping of the cold plate. This is the last variable needed to solve for the total resistance of the thermal resistance network

The following equation combines the convective thermal resistances from the cold plates piping as well as the cold plates conductive resistance in series to yield [5],

$$R_{total} = \left(\frac{1}{(hA)1} + \frac{1}{(hA)2}\right) + \frac{L}{KA_{cond}}.$$
 (7)

In Equation 7, h is the heat transfer coefficient of the fluid through the piping, A is the cylindrical surface area of the pipe, L is the thickness of the cold plate itself, K is the thermal conductivity of the cold plate and A_{cond} is the effective conductive cross-sectional area. The cold plate in the proposed design features two piping systems that run concentrically to each other. This increases heat transfer out of the system due to the increased amount of fluid being passed through

the cold plate. The inclusion of two piping systems is reflected in equation 9 as there are two convective thermal resistances being summed along with the conductive thermal resistance.

Now that the equations have put in place, these steps can now be followed through using different fluids with different properties. In this case the two fluids used were water, and a hydrocarbon refrigerant, R-134a. The fluids and calculated values are listed below in Table 1.

Fluid	Temp.	Rho	Mu	Re	Pr	Nu	h	$R_{coldplate}$
	[C]	[kg/m^3]	[Pa-S]				[W/m^2-K]	[K/W]
DI	5	997	8.9E-4	56907.2	7.56	393	18566.9	0.0005
Water								
R-134a	-25	1373.4	406E-6	171844.1	4.69	802.166	6505.76	0.00132

Table 1. Fluids and calculated values.

The design that uses water as a working fluid is the most effective with a resistance of 0.0005 K/W. The hydrocarbon, R-134a, had a total thermal resistance of 0.00132. The thermal resistance of the cold plate using water is 37.6% of the cold plates using the hydrocarbon as a working fluid. While this is promising, unfortunately the PEBB must also be electrically insulated. Water is electrically conductive meaning when the heated water has passed through the cold plate and heads to the chiller to be re-cooled, it causes the PEBB to be no longer insulated. The hydrocarbon fluid, unlike the water, is electrically insulating. Thus, a tradeoff must be made between the cooling efficiency of the working fluid and the need for the fluid to be electrically insulating. Another solution would be to use deionized water. Deionized water would meet the requirement for an electrically insulating fluid while having excellent heat transfer properties. The

performance on the cold plate is heavily dependent on the choice of working fluid. If deionized water is chosen, the thermal resistance of the cold plate is 0.0005 K/W. If a common refrigerant such as R-134a is chosen, the thermal resistance jumps to 0.00132 K/W.

Finally, the total thermal resistance of the system can be calculated by adding the resistance of the module, the thermal pad and the cold plate together, as resistors in series. This summation,

$$R_{total} = R_{module} + R_{thermalpad} + R_{coldplate}, \tag{8}$$

yields a total thermal resistance of 0.6105 K/W. This means for every Watt of heat flux introduced into the system, the temperature difference between the junction of a single die to the top of the cold plate is 0.6105 K.

The PEBB has two main operating scenarios. The first is when the 10 KW heat load is spread over all 72 dice uniformly such that each die is subjected to a 138.89 W heat load. The second scenario is when 80% of the heat load is subjected to half of the dice and 20% of the heat load is subjected to the other half resulting in heat loads of 222.22 W and 55.56 W respectively. To see how the system will react to such loads, the equation [5],

$$Q = \frac{\Delta T}{R_{total}},\tag{10}$$

is used. Here, Q is the heat load on a single die in watts, ΔT is the temperature difference between the junction and the top of the cold plate per die, and R_{total} is the thermal resistance of a single die from junction to cold plate. Table 2 below shows the cooling performance of the system for each load case and working fluid.

Q	Working Fluid	R_{total}	ΔT
[W]		[K/W]	[K]
222.22	DI Water	0.6105	135.65
138.89	DI Water	0.6105	84.79
55.56	DI Water	0.6105	33.92
222.22	R-134a	0.6113	138.85
138.89	R-134a	0.6113	84.91
55.56	R-134a	0.6113	33.97

Table 2. Cooling performance of the system for each load case and working fluid.

These results show that at the highest load case the deionized water is 2% more effective, at the uniform load case the water is 1% more effective, and at the lowest load case there is a negligible difference between the cold plate using water and the cold plate using R-134a.

4. Simulated Models

One common technique to verify thermal systems analysis uses Computational Fluid Dynamics (CFD) simulations. CFD simulations are useful because they allow for comprehensive three-dimensional visualizations of systems under load cases that theoretical analysis, as described in Section 3, cannot supply. However, it is important to realize that simulations are only as good as their set-up. Thus, it is crucial that exact initial and boundary conditions are set so that the simulation can solve the correct load cases. As with the theoretical analysis above, four cases were simulated:

- uniform thermal loading, with working fluid of water and R-134a, and
- nonuniform thermal loading with water and R-134a as the working fluid.

A fine, tetrahedral mesh was used for this application. In future simulations, with a more powerful software, a hexagonal mesh would allow for more accurate convergence; however, during the scope of this paper, this was not possible. Exact parameters and loading conditions for each simulated case can be seen below in Table 3.

Load Type	Fluid	Pressure	Inlet	Inlet	Prandtl	Specific	Run
		[atm]	Velocity	Temp.		Heat	Time
			[m/s]	[C]		[J/kg-K]	[s]
Uniform	DI Water	1	4	5	7	4180	500
Nonuniform	DI Water	1	4	5	7	4180	500
Uniform	R-134a	1	4	-25	4.69	1282.7	500
Nonuniform	R-134a	1	4	-25	4.69	1282.7	500

Table 3. Parameters and loading conditions for each simulated case.

The simulations were then run yielding the results seen in Figures 14-17 and detailed below in Table 4.

Load	Fluid	T_{avg}^{die}	$T_{avg}^{coldplate}$	ΔT	R_{th}
[W]		[C]	[C]	[C]	[K/W]
222.22	DI Water	161.2	23.51	137.69	0.62
138.89	DI Water	107.8	23.4	84.4	0.61
55.56	DI Water	58.17	23.51	34.66	0.62
222.22	R-134a	160.3	15.56	144.74	0.65
138.89	R-134a	110.3	15.46	94.84	0.68
55.56	R-134a	53.14	15.56	37.58	0.68

Table 4. Simulation results.

These results, like the theoretical analysis, demonstrate the effectiveness of liquid cooling systems no matter the working fluid selected. As with the theoretical results, the cooling system that used water maintained lower thermal resistances and lower temperature differences between the junction and cold plate.

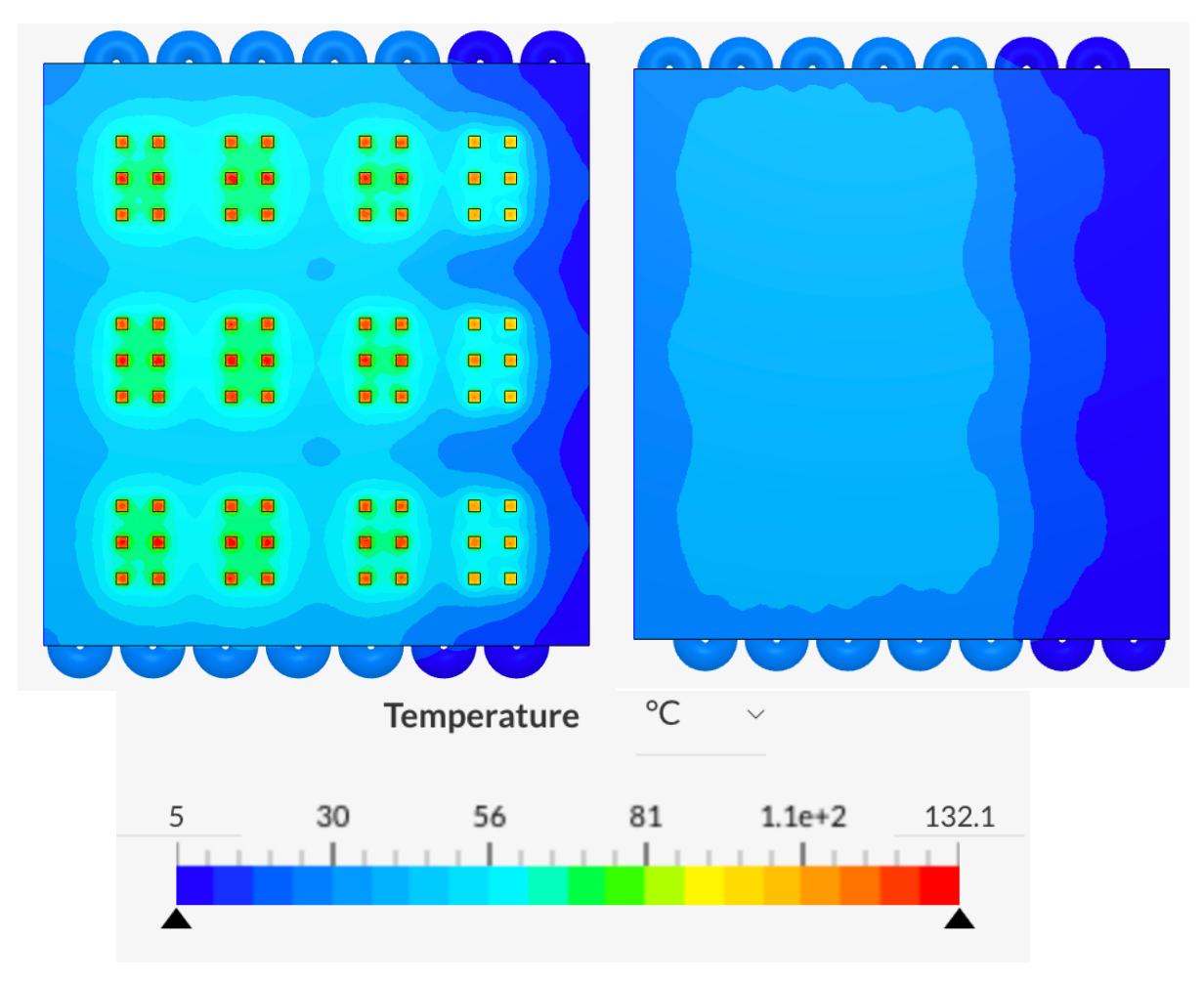


Figure 14: Water acting as working fluid with 138.89 W Uniform Load across 72 dice.

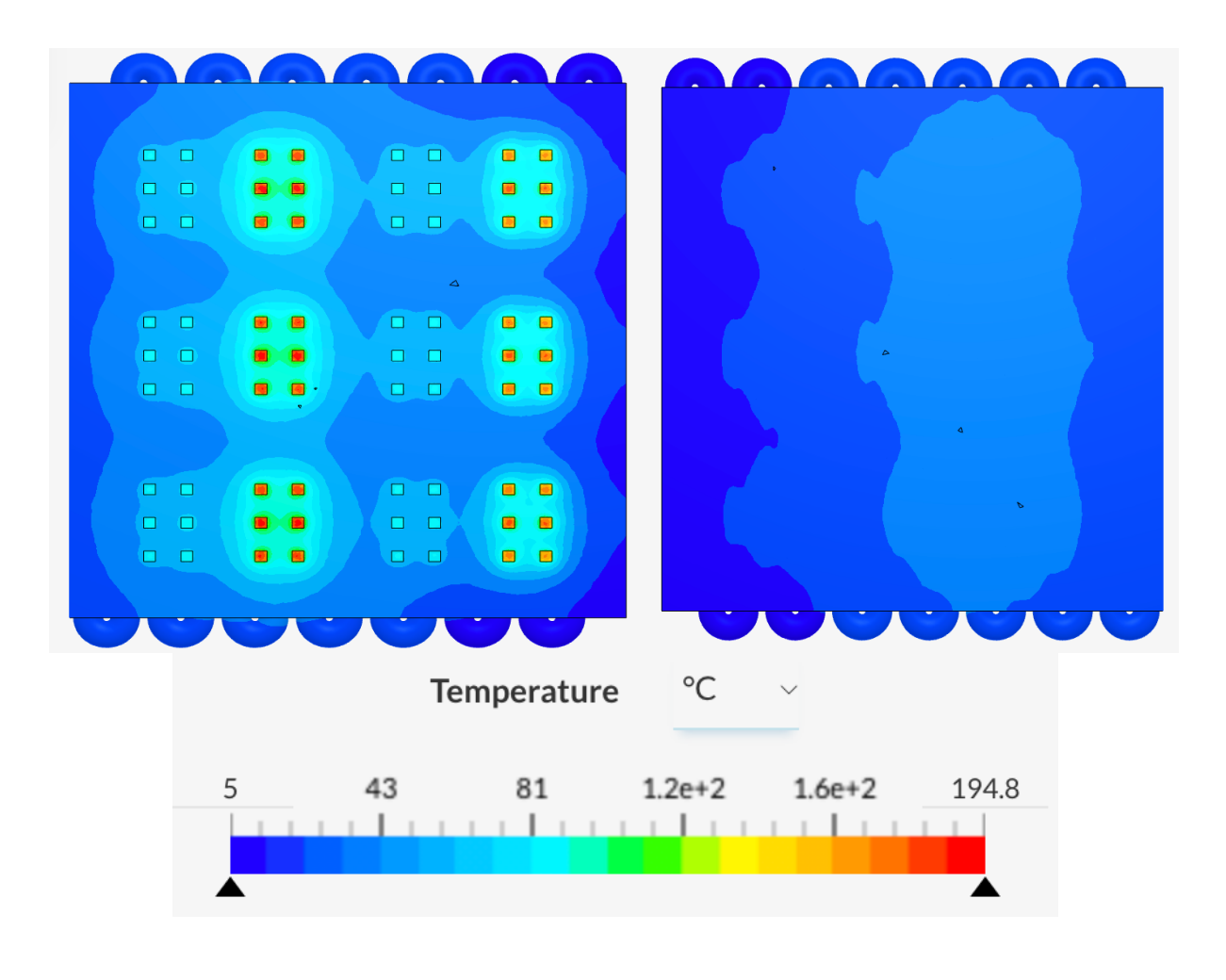


Figure 15: Water acting as working fluid with 222.22 W/55.56W Nonuniform Load across 72 dice.

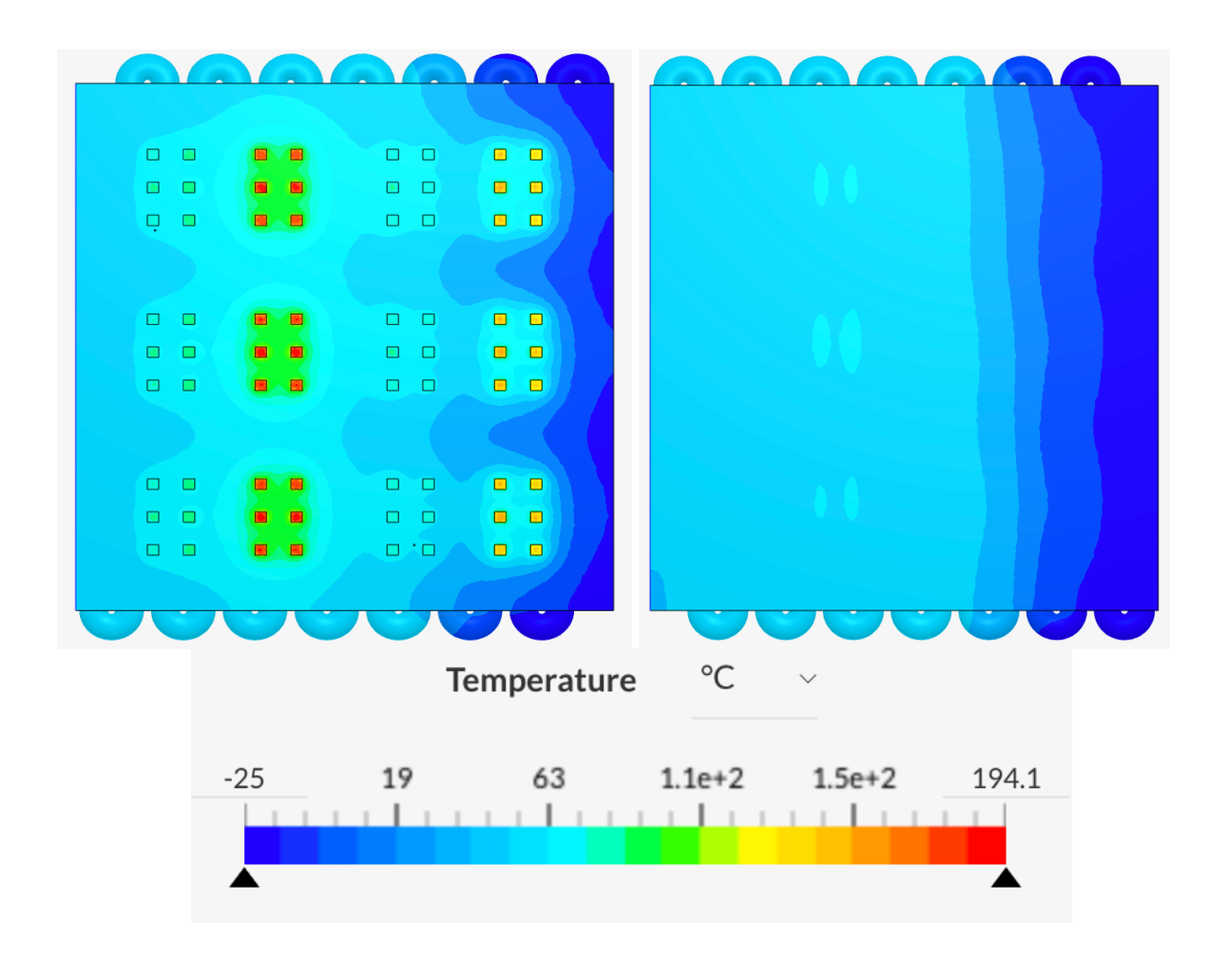


Figure 16: R-134a acting as working fluid with 222.22 W/55.56W Nonuniform Load across 72 dice.

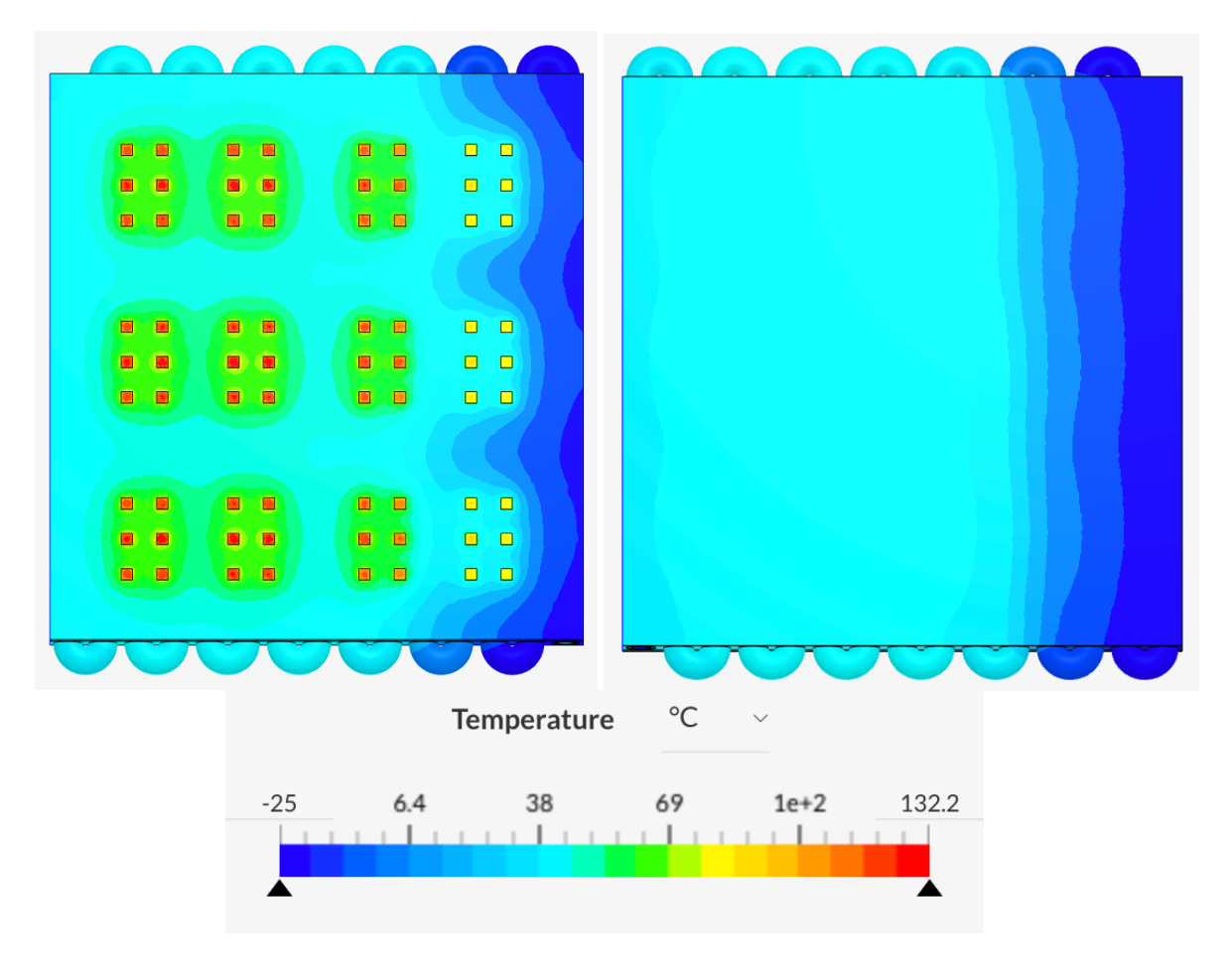


Figure 17: R-134a acting as working fluid with 138.89 W Uniform Load across 72 dice.

5. Results and Discussion

The analytical modeling as well as the simulation results both yield promising results for the performance of the proposed liquid cooling solution. In order to evaluate both results they must be compared to each other, as well as to the performance of the air-cooled design used currently. First, the analytical results will be compared to the simulation results with water and R-134a used as the working fluids. These comparisons can be seen below in Table 5 and use thermal resistance from die to cold plate as the metric.

DI Water	R-134a	DI Water	R-134a	DI Water	R-134a
Resistance	Resistance	Resistance	Resistance	Comparison	Comparison
(AM)	(AM)	(SIM)	(SIM)	(AM/SIM)	(AM/SIM)
0.6105 K/W	0.6113 K/W	0.61 K/W	0.68 K/W	1.0008	0.89897

Table 5. Comparison of results.

These results show that in the case of water, the simulation and analytical models yielded virtually identical results, however in the case of the R-134a, the results differed by approximately 10%. This is promising as it shows high levels of agreement between the simulation and analytical models demonstrating through understanding of the cooling systems behavior. The 10% difference in the R-134a case occurs due to the fact that in the analytical model, the changes in properties such as viscosity of R-134a due to temperature changes are not accounted for while in the simulation, they are. R-134a is a hydrocarbon whose various thermal properties are heavily affected by temperature. This results in the small difference seen between the analytical and simulation results.

Now the liquid-cooled and air-cooled systems must be compared. Going forward, to compare the effectiveness of using water, R-124a, and air as working fluids, the water resistance value from the analytical model will be used, the R-134a resistance value from the simulation will be used, and the value provided by Virginia Tech for the air-cooled thermal resistance will be used. The comparisons between working fluids can be seen in Table 6.

DI Water	R-134a	Air	Air-Water Comparison	Air-R-134a Comparison
Resistance	Resistance	Resistance	(% difference)	(% difference)
(K/W)	(K/W)	(K/W)		
0.6105	0.68	1	38.95	32

Table 6. Comparisons between working fluids.

The values shown in Table 6 demonstrate the effectiveness of liquid cooling as with both water and R-134a the thermal resistance of the total system is more than 30% less than that of the air-cooled system. The difference in effectiveness of the liquid system using water versus R-134a is only 10% and indicated that no matter the working fluid, cooling effectiveness does not differ very much. Choosing between Water and R-134a in the final system will come down to other factors such as ease of implementation and other components such as chillers, piping, and pumps.

6. Conclusions and Future Work

In this thesis it has been shown that the proposed cooling paradigm is a viable solution to the proposed problem. Through the use of analytical models and computational fluid dynamics simulations, it has been shown that the proposed power electronics elements can be maintained at an acceptable temperature using either water or refrigerant as a cooling medium. Further, the structural analysis has demonstrated that the pressure required for compressing the thermal pad is achievable and the PEBB can be designed to withstand the pressure within the weight and size constraints. It was determined that the majority of the thermal resistance occurs within the PEBB structure itself. Spreading of the heat using, for example, vapor chambers integrated into the PEBB structure will enhance heat transfer and improve the performance of the cooling system. Further work must be done to experiment with heat spreading techniques and design for integration into the PEBB's electronics and internal components.

A separate concern that must be addressed in the future is that, although heat transfer is enhanced by placing the cooling element vertically above the heat-producing element, for security of the PEBBs in a shipboard environment, especially in heavy seas, it may make sense to change the planned cooling system by inverting the PEBB units and placing them on top of the cold plates.

Although the results in this thesis demonstrate effectiveness of liquid cooling and the proposed design, the analytical and simulated models must be confirmed experimentally. Next steps include creating and testing an appropriately scaled physical mockup of the proposed system. This will allow for further validation of the liquid cooling design allowing the project to move forward.

References

- [1] 2021, "Gap Fillers vs. Thermal Pads", LORD Corp [Online]. Available: https://www.lord.com/products-and-solutions/electronic-materials/thermal-management-materials/gap-fillers-vs-thermal-pads. [Accessed: 16- Feb- 2021].
- [2] 2021, "TG-A1780 Ultra Soft Thermal Pad | PRODUCTS | T-global Technology Professional thermal solution, heat solution, heat dissipation, thermal engineering solution expert", Tglobalcorp.com [Online]. Available: https://www.tglobalcorp.com/tg-a1780-ultra-soft-thermal-conductive-pad. [Accessed: 16- Feb- 2021].
- [3] 2021, "Aluminum Nitride (AlN) Ceramic Precision Ceramics USA", Precision Ceramics USA [Online]. Available: https://precision-ceramics.com/materials/aluminum-nitride/. [Accessed: 16- Feb- 2021].
- [4] Guenin, B., 2021, "The 45° Heat Spreading Angle An Urban Legend? | Electronics Cooling", Electronics Cooling [Online]. Available: https://www.electronics-cooling.com/2003/11/the-45-heat-spreading-angle-an-urban-legend/. [Accessed: 16- Feb- 2021].
- [5] Cravalho, E., Smith, Jr., J., Brisson, J., and McKinley, G., 1997, 2.006 Thermal Fluids Engineering.
- [6] S. Mocevic, J. Yu, Y. Xu, J. Stewart, J. Wang, I. Cvetkovic, D. Dong, R. Burgos, and D. Boroyevich, 2020, "Power-cell design and assessment methodology based on a high-current 10 kV SiC MOSFET half-bridge module," IEEE Journal of Emerging and Selected Topics in Power Electronics.